

Improving curve skeletons of tubular volumes

Florent Grélard, Fabien Baldacci, Anne Vialard and Jean-Philippe Domenger

Univ. Bordeaux, LaBRI, UMR 5800, F-33400 Talence, France

CNRS, LaBRI, UMR 5800, F-33400 Talence, France

e-mail: florent.grelard@labri.fr

Abstract— Curve-skeletons encode both geometrical and topological information of 3D volumes (sets of voxels), and are key to many applications. However, due to the complexity and variability of the shapes, there is a variety of algorithms yielding skeletons suitable for certain objects, but inappropriate for others. In this article, we are interested in filtering skeletons of digital tubular objects with varying-diameter and junctions, resulting from the segmentation of organs (airway-trees, vessels). Existing skeletons might not be centered or contain faulty branches. For medical applications such as virtual endoscopy or cross-section estimation, post-processing steps are applied in order to prune the spurious branches and smooth the skeleton. State-of-the-art methods for pruning are insufficient with respect to varying-diameter tubes. We propose a new approach to prune irrelevant skeleton branches, and to recenter the skeleton inside the shape.

Keywords— Pruning, Recentering, 3D curve-skeleton

I. INTRODUCTION

Curve-skeletons are sets of curves, also referred to as centerlines which are simplifications of shapes with several applications in image analysis. For instance, skeletons are useful to match two shapes [1], and for shape decomposition [2]. It is also prevalent in medical applications, with applications ranging from virtual endoscopy [3] to geometrical measurements, such as tortuosity [4] or tangent estimation [5]. A lot of skeletonization algorithms have been proposed since there is not a unique method which is satisfying for all shapes. In this article, we focus on shapes representing tubular organs such as airway-trees, blood vessels or neurons. The applications range from geometrical estimation to shape matching. In this context, the skeleton must be as “clean” as possible, meaning it is centered inside the tubular parts, complete (every tubular part has a corresponding branch in the skeleton), and without faulty branches. Satisfying these properties is not achievable even with the most recent methods for our shapes (see [6] for explanations). Some algorithms yield incomplete skeletons, or with faulty branches (see Figs. 1b and 1c), while others provide results which are not centered or which are unsatisfactory with respect to junctions (i.e. areas where several branches intersect, see Fig. 1a).

Spurious branches in the skeleton appear as a result of small irregularities on the object’s surface which are kept through the skeletonization process. Pruning consists in the removal of irrelevant parts of the skeleton, yielding a skeleton representing the original shape more aptly. Once all the extra branches have been removed, each tubular part of the organ is represented by a unique branch, allowing the analysis of the organ. One of the main challenges of pruning approaches is to remove

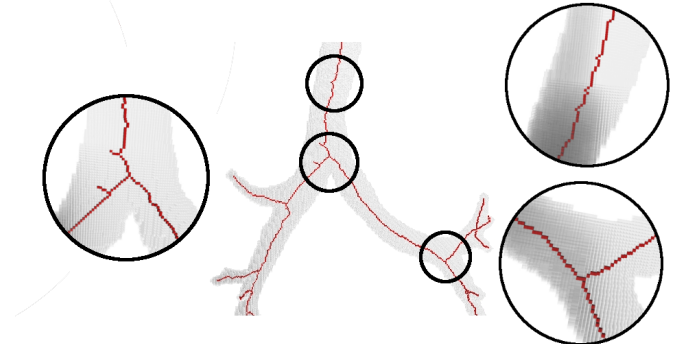


Fig. 2: Skeleton (in red) of an airway-tree (in grey). The skeleton contains spurious branches (see closeup on the left), zigzags and is not centered (see closeups on the right).

all spurious branches while keeping meaningful ones. Most pruning methods define a significance measure based on the branch length. This approach is not sufficient for varying-diameter shapes, where spurious branches have various length (see Fig. 2).

The last filtering step consists in recentering the skeleton. Indeed, not all skeletons are centered or smooth inside the shape (see closeups in Fig. 2), impacting geometrical analyses and virtual endoscopy. For example, if the diameter of the tube is evaluated as the distance transform value from a non-centered skeleton point, it will not correspond to the expected value.

In this paper, an original approach to prune and recenter any given skeleton is proposed. The paper is organized as follows. In Section II we present state-of-the-art skeletonization algorithms, and existing pruning and recentering methods. In Section III, we recall the basics of orthogonal plane computation introduced in a previous work. Section IV describes our pruning method. In Section V, we compute smooth and recentered skeletons. Results on synthetic and real data are described and discussed in Section VI.

II. RELATED WORKS

There are two main classes of algorithms producing **3D curve-skeletons** (a) thinning algorithms (b) distance field or general field algorithms [9]. Two representative examples of *Thinning methods* are presented in [7] and [10]. The former computes the skeleton on any given 3D object whereas the latter is dedicated to tubular shapes. They both consist in

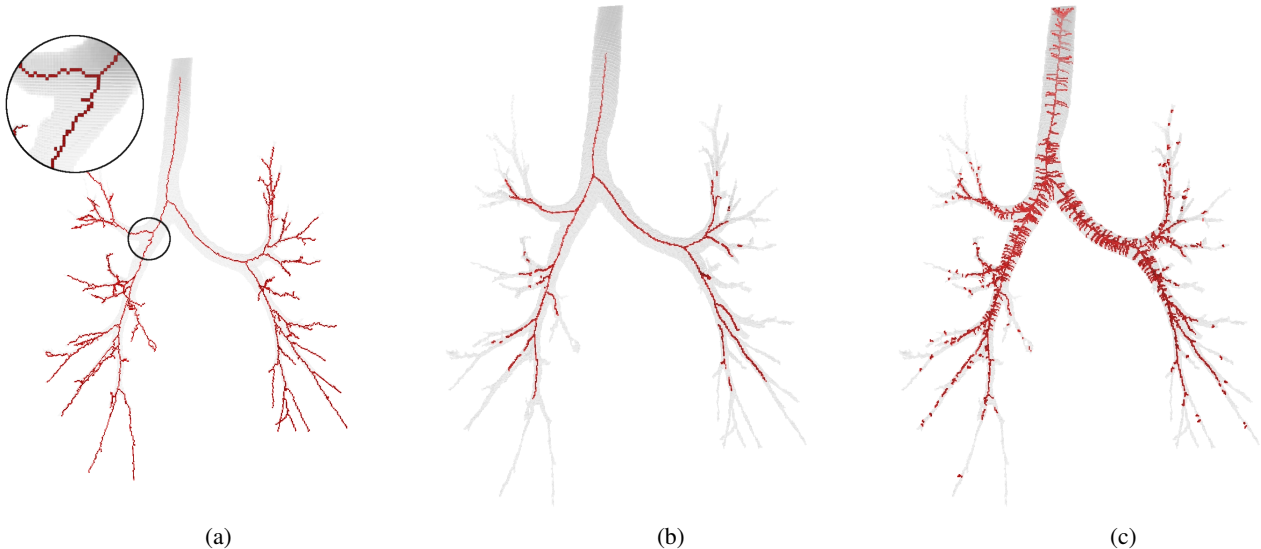


Fig. 1: (a) Skeleton computed using the method described in [7]: skeleton contains small faulty branches, as well as non-centered points, see closeup view. (b) (c) Skeleton computed using potential field [8], with different parameter values. Obtaining a skeleton containing all the branches in the volume as well as no faulty branches is not possible.

removing layers of voxels while preserving the topology of the initial shape. The main drawback of thinning algorithms is they can yield skeletons containing spurious branches, resulting from irregularities on the surface kept throughout the skeletonization process (see Fig. 1a). *Potential field* methods generally produce very smooth skeletons. For instance, in [8], [11] the skeleton is extracted from a potential field computed on the volume. A force is applied on each point of the boundary towards the interior of the shape. The skeleton points are the points where the resulting vector field vanishes. The main drawback of this kind of algorithm is that obtaining a skeleton with no faulty branches as well as complete is impossible in the case of varying-diameter objects (see Fig. 1b and 1c).

Pruning consists in removing faulty branches while keeping meaningful ones with respect to the object. The general idea is to design a significance measure which captures the relevance of a branch [12]. Most of these measures aim at determining if a branch stems from a small irregularity on the surface. A recent work describes a hierarchical pruning method of 3D-curve skeletons [13]. The authors use the combination of four significance measures : a length criterion, a criterion estimating whether the branch is centered, and two criteria involving the amount of information the branch encodes in the shape. The thresholds for each criterion is set automatically by averaging measures over branches. This method has two main drawbacks with respect to our tube-shaped volumes. First, one criterion is relying on centeredness of the branch. However, this property is not always guaranteed (see Fig. 3). Second, using the average of the significance measure is not relevant in the context of varying-diameter shapes.

Another post-processing step consists in **recentering** the skeleton in order to make robust geometrical measurements of

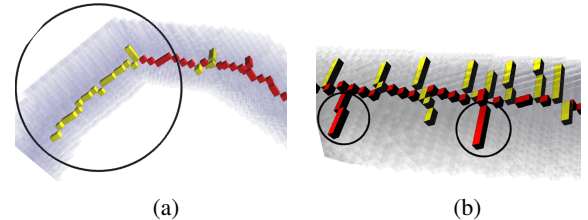


Fig. 3: Pruned branches (in yellow) of a skeleton computed using [8]. The pruning method is described in [13]. The centeredness criterion leads to errors: (a) relevant branches are pruned (circled) and (b) spurious branches are kept.

the shape. In [14], 3D curve-skeletons skeletons are smoothed and recentered. The method is based on the computation of the set of the maximal balls centered at each point of the input skeleton. A subset of the maximal balls, which is representative of the shape is kept. The resulting skeleton is composed of the centers of these balls linked by splines. Although the presented approach is interesting in the context of noisy data, it can discard small geometrical features. The authors in [15] describe another approach to recenter a skeleton inside a shape. The tangent vector, defined here as the difference between a skeleton point and its direct neighbor, is computed at each point of the input (non-centered) skeleton. The tangent vector defines an orthogonal plane which is intersected with the volume. A centroid of the resulting cross-section is chosen as the new recentered skeleton point. The main drawback of this method is that the tangent computation is very sensitive to irregularities in the skeleton, and junctions are not properly processed.

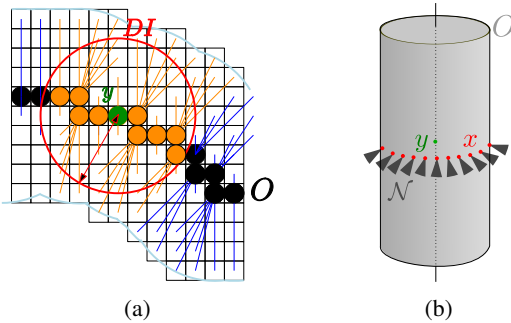


Fig. 4: (a) 2D digital object (in black, O) and computation of the VCM around y by integration of Voronoï vectors (in orange) in the domain of integration, denoted by DI . (b) The orthogonal plane at y corresponds to the sum of the contribution of normal cones (in dark gray, denoted by N)

III. BACKGROUND

In [16], we described a way to compute orthogonal planes from a voxel set. Our method is based on a Voronoï covariance measure (VCM). The VCM is a normal estimator defined on volumes in [17]. The normal is given by analyzing the local shape of Voronoï cells through the computation of their covariance matrices. The normal corresponds to the eigenvector with the largest eigenvalue in the covariance matrix. More precisely, the VCM computes at a point y in a digital object O a covariance matrix of vectors between points in a domain of integration DI centered at y and the sites of their respective Voronoï cells, denoted by $p_O(x)$ (see Fig. 4a). The covariance matrix is given as:

$$\mathcal{V}_O(y) = \sum_{x \in DI_O(y)} (x - p_O(x))(x - p_O(x))^t$$

where DI is generally a ball of radius r .

In [16], we compute orthogonal planes on a 3D object by summing the contribution of all the normal cones N in the domain of integration (see Fig. 4b). The orthogonal plane is defined as the plane spanned by the two eigenvectors with the highest eigenvalues in the covariance matrix, i.e. those which define the normal cone. The VCM is defined on any compact, meaning the orthogonal planes can be computed from a curve (skeleton) or directly from the object.

In [6], we used VCM to compute a curve-skeleton on certain tubular objects for which junctions can be detected using a curvature criterion. We designed a tracking algorithm where the skeleton points correspond to the centers of mass of the intersection between the orthogonal plane and the object. A similar idea is used in the recentering scheme we propose.

IV. PRUNING

As explained in Section II, skeletons of tubular objects have irrelevant branches due to surface irregularities. Those branches are not aligned with the tube's axis. In this section,

we propose a new significance measure based on orthogonal plane computation to estimate the deviation of a skeleton branch from the tubular object direction.

The significance measure consists in measuring the angle α formed by the two orthogonal planes defined, on one hand by the curve and, on the other hand by the volume. The orthogonal plane normal of an undesired branch is directed at the object's surface, whereas its volumetric counterpart is along the shape. The angle formed by the two planes for spurious branches is large, whereas it is low for meaningful branches (see Fig. 5a).

Orthogonal planes on the curve and the volume are computed with VCM at each point in the branch (see Section III). In order to obtain a robust estimation of the orthogonal plane, it is important to choose the right value for the size of the domain of integration r of the VCM. This parameter defines the number of neighbors taken into account for the computation of the covariance matrix. Regarding the computation of the orthogonal plane from the curve, r depends on the branch length. Indeed, a downscaled version of a given curve should have a lower r , in order to get into account only relevant local information. Experimentally, we choose r as a fraction of the branch length.

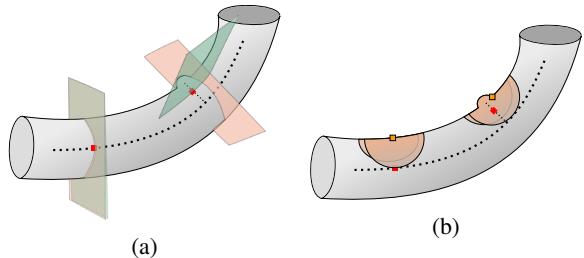


Fig. 5: (a) Difference between orthogonal planes computed from the curve (green plane) and the volume (pale red plane). On the left, the two orthogonal planes overlap, because the skeleton is aligned with the tube. On the right, the plane computed on a spurious branch is highly deviated compared to the one computed on the volume. (b) Domains of integration (in pale orange) centered at the closest point (in orange) from the skeleton point (in red) for the orthogonal plane computation on the volume.

Regarding the computation on the volume, it is necessary to determine surface points from the branch which accurately capture the object's shape. The domain of integration of the VCM is centered at the closest point on the surface. Then, the domain of integration should integrate sufficient surface points to account for the local shape of the object. It is not necessary to integrate the full perimeter of the tube starting from this point, a subset is generally enough. It results r is chosen as the maximal distance transform (DT) value in the branch, which, in the case of a perfectly circular tube consists in integrating half the perimeter of the tube (see Fig. 5b). The angle difference α is computed for each point in the branch. The average angle for a branch allows to discard it

or keep it according to a threshold. Setting a global threshold is not a problem in this case since the significance measure is independent of the local scale of the shape. The choice of the threshold is discussed in Section VI.

All branches in the skeleton are analyzed during the pruning procedure. Only those having a significance measure above a given threshold and preserving the same number of connected components as in the initial skeleton when removed are deleted. The skeleton is modified and updated when a branch is deleted. Computation of the significance measure is done on each branch of the updated skeleton until no branch can be removed. This ensures that the pruned skeleton is not disconnected, and that all spurious branches across the skeleton are deleted.

V. RECENTERING

Our recentering approach is based on orthogonal plane computation, as described in Section III. Only previously pruned skeletons are recentered.

Our **method** is the following: new recentered points correspond to the centers of mass of the cross-sections computed at each point of the input skeleton. Each branch is processed independently. The recentered skeleton points might be disconnected due to the fact that points are shifted from the input skeleton during the recentering procedure. However, the initial skeleton is connected, which implies that computed orthogonal planes are close from one another. As a result, recentered points remain close (generally at most one point apart from each other). For this reason, each pair of disconnected points is linked by a small digital segment, without altering the centeredness of the skeleton.

Junctions consist in the intersection of three or more tubes and must be handled specifically. In the following, only junctions consisting of three tubes are described for the sake of simplicity. Junction parts are not tubular as they are not elongated in one direction. In such areas, centers of mass of cross-sections are not meaningful.

The goal is to extract tubular sub-volumes in junctions, from which centers of mass are meaningful (see Fig. 6a). The junction can be regarded as the division of a parent tube into two children. Each child branch can be associated to its parent branch, the union of both being a tubular object. Orthogonal planes are used to find cutting planes to compute these sub-volumes. In a pruned skeleton, branching points (i.e. points having at least three neighbors) are in close correspondence with junction areas in the volume, and interesting cutting planes are in the neighborhood of branching points in the skeleton.

For each edge around a branching point b , the cutting plane should be positioned at a point where it delineates the tubular branch from the junction area. Orthogonal planes computed near branching points in a child branch intersect the other child branch (see Fig. 6b). In other words, the area of the cross-section is much larger in the junction than in the child branch

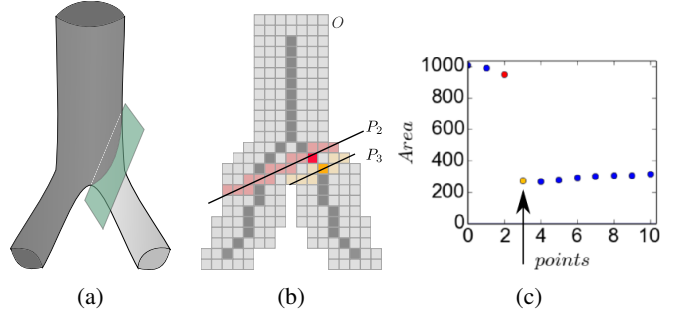


Fig. 6: (a) Computation of a sub-volume. The cutting plane (in green) isolates the sub-volume, consisting in a parent and a child branch (dark grey), from another child (light grey). (b) Computation of orthogonal planes at two points on the same edge. The number of volume points in the plane (i.e. the area) varies a lot in junctions. (b) Typical area variation (y-axis) observed along an edge. The cutting point is the point where the area variation is the highest (see arrow).

(see Fig. 6c). The cutting point corresponds to the point where the area variation is the largest. The area A at p is computed as the number of points in the intersection between the orthogonal plane and the volume. To study the area variation, we study the factor $\sigma(x)$ along the edge E .

$$\sigma(x) = \max_{y \in \mathcal{N}_E(x)} \frac{A(y)}{A(x)}$$

where $\mathcal{N}_E(x)$ is the 26-neighborhood of x in E .

Then the cutting point c in the edge E is defined as $c = \max_{x \in E} \sigma(x)$. In a junction, only the cutting points of the child branches and their corresponding cutting planes are considered.

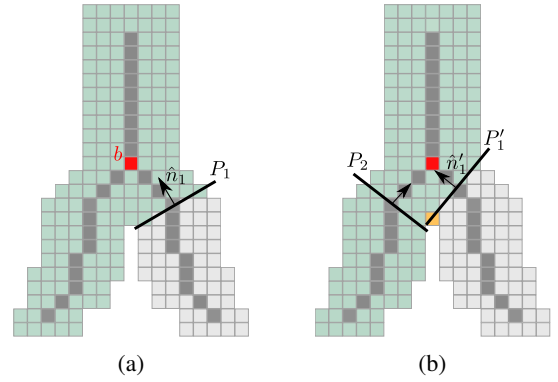


Fig. 7: (a) Sub-volume (in green) computed using orthogonal planes on an input skeleton. (b) Sub-volume (in green) obtained after rotating the plane P_1 around the center (in orange) so that the new cutting plane P'_1 is orthogonal to the plane P_2 located in the other child branch.

However, orthogonal planes are not proper delineations, as child branches are not aligned with parent branches (see Fig. 7a). The idea is to align the plane with the axis of the other

child tube. The direction of the axis is given by the orthogonal plane normal (i.e. the tangent to the curve) computed in the other child tube. Thus, the first cutting plane is rotated so that it is orthogonal to the other cutting plane. Let P_1 and P_2 be the two cutting planes at a junction and \hat{n}_1 and \hat{n}_2 their respective normals. Then, \hat{n}_1 is rotated so that it is made orthogonal to \hat{n}_2 . The direction of the rotation axis is given as the cross-product of the two normals. Finally, the cutting plane normal is $\hat{n}'_1 = (\hat{n}_1 \wedge \hat{n}_2) \wedge \hat{n}_2$. The rotation axis is placed on a point in $P_1 \cap O$ minimizing the distance to P_2 . After rotation of the planes, two tubular sub-volumes can be isolated from each branching point b . First, the volume is restricted due to computational considerations. Let $B(p, r)$ be a ball of radius r and centered in p . The restricted area of computation O' is defined as $B(b, r) \cap O$ where r corresponds to the maximum of half the edge size (in order to analyze the edge locally). The ball might contain different connected components, only the component containing b is kept.

Second, the two sub-volumes S_1 and S_2 are defined as all volume points in O' above their respective cutting planes. Finally, S_1 and S_2 are tubular structures, and the skeleton is recentered by computing the centers of mass in the sub-volumes.

VI. RESULTS

In this section, our pruning and recentering approaches are evaluated. They have been implemented using the DGtal library [18].

Skeletons have been generated using the algorithm described in [8] with parameters chosen specifically to yield spurious branches. Our pruning scheme is then applied on the skeletons. Faulty branches are inspected and classified visually. In the following, interesting experimental values for the angle threshold have been found to be in the range of 20 to 35 degrees. Below 20 degrees, relevant branches might get deleted due to the fact that orthogonal planes computed on the curve and on the volume differ slightly. Results on four varying-diameter tubular objects are presented in Fig. 8.

The quality of a pruning approach is determined by the number of spurious branches it deletes while preserving the maximum number of relevant branches. Out of the four initial skeletons, only one spurious branch is not deleted (see close-ups in Fig. 9). This particular spurious branch is aligned with the tube's axis, thus it cannot be discarded using our method. Spurious branches intersecting with one another and forming a cycle can also be deleted (see rightmost cycled area in Fig. 9). Our pruning approach also preserves relevant branches. Only small peripheral branches might get removed, because there is not enough information to estimate the significance measure robustly (see Fig 9c). On average, among the four volumes presented above, 3.75 small peripheral branches are removed. Due to their small length, these branches are not suitable to make geometrical measurements or to perform virtual endoscopy, so their removal does not impede further analysis.

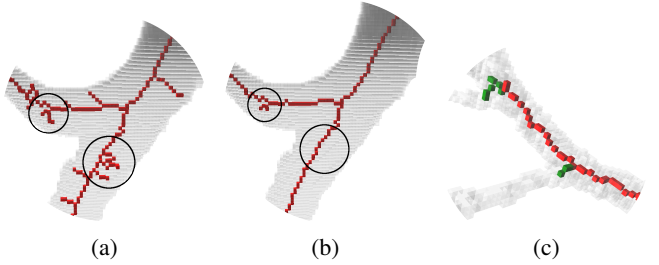


Fig. 9: (a) Closeup on spurious branches in the initial skeleton intersecting with one another (circled in black). (b) On the leftmost circled area, one spurious branch remains. On the right, the cycle is properly removed. (c) Small relevant branches removed using our approach (in green).

Table 1: Comparison of our pruning method to the state-of-the-art method in [13]. Four measures are used to assess the completeness and sensitivity of our method compared to the state-of-the-art. The number of spurious branches deleted by the existing method and not deleted by ours (denoted by Err_{VCM1}); the number of spurious branches deleted by our method but not deleted by the existing one (Err_{ST1}); the number of relevant branches deleted by the existing one, but preserved by ours (Err_{ST2}); and the number of relevant branches deleted by our method but preserved by the other (Err_{VCM2}). These measures are computed on the four volumes of Fig. 8.

Volumes Fig.	8a	8b	8c	8d
Err _{VCM1}	1	0	0	0
Err _{VCM2}	4	1	3	1
Err _{ST1}	6	4	2	3
Err _{ST2}	15	3	9	14

Furthermore, our method is compared to the pruning approach introduced in [13]. Results in Table 1 show our method is more complete because it deletes more spurious branches than the existing method (see Err_{ST1}) and the existing method does not remove more branches (see low values for Err_{VCM1}). Moreover, our method is more sensitive, because it preserves more relevant branches (see Err_{VCM2} and Err_{ST2}).

The recentering procedure was tested on non-centered skeletons generated using the thinning algorithm described in [10]. Results on real data (airway-tree segmentation) show the skeleton is centered in junctions, and properly smooth zigzags (see Fig. 10). However, our method is not robust for junctions between small tubes (see Fig. 10h). The cutting planes are not properly positioned since area variations are not as significative for tubes with low diameter. This problem is not of major importance since we can keep the original skeleton which is close to the centerline by definition in the case of small diameter tubes.

VII. CONCLUSION AND PROSPECTS

In this article, we have presented two methods to improve curve-skeletons on tubular objects. Our pruning method is both

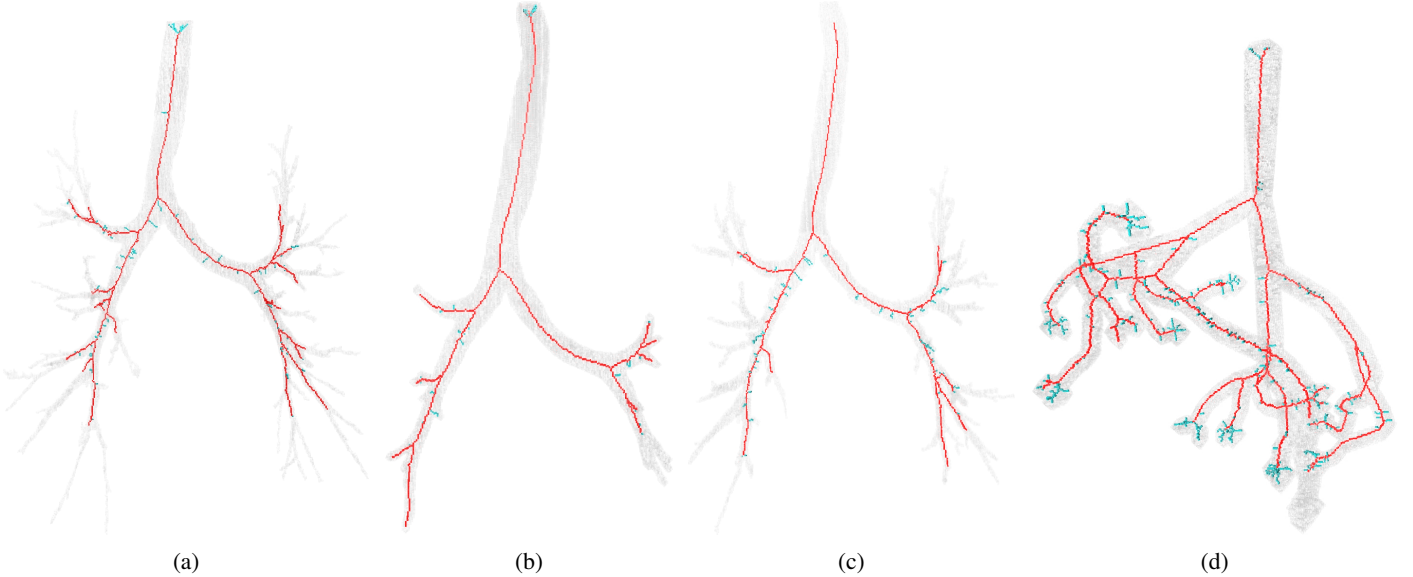


Fig. 8: (a)-(d) Resulting skeletons (in red) with pruned branches (in cyan). Initial skeletons were generated using [8] on various varying-diameter tubular objects.

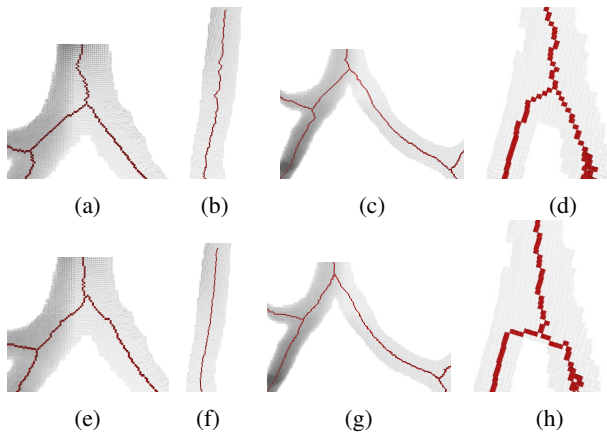


Fig. 10: (a)-(d) Initial non-centered skeletons generated using [10] on airway-tree segmentations. (e)-(h) Corresponding resulting recentered skeletons. (d) and (h) shows a case where the skeleton is not properly recentered by our method in small-diameter tubes.

more complete and sensitive than the existing method, and is close to the expected results with respect to the removal of spurious branches. Moreover, our significance measure is not dependent on the local scale of the object, which makes it convenient to use for varying-diameter tubular objects. Pruned skeletons are recentered robustly, facilitating tasks such as geometrical measurements or endoscopy. Our recentering method might be faulty in certain parts of the volume, due to the cutting plane not being properly positioned. We aim at improving this aspect in the future.

REFERENCES

- [1] X. Bai and L. J. Latecki, “Path similarity skeleton graph matching,” *IEEE Trans. PAMI*, vol. 30, no. 7, 2008.
- [2] L. Serino, C. Arcelli, and G. S. di Baja, “From the zones of influence of skeleton branch points to meaningful object parts,” in *DGCI*, pp. 131–142, 2013.
- [3] C. Bauer and H. Bischof, “Extracting curve skeletons from gray value images for virtual endoscopy,” in *MIAR*, 2008.
- [4] S. L. et al., “Three-dimensional quantification of capillary networks in healthy and cancerous tissues of two mice,” *Microvascular Research*, vol. 84, no. 3, pp. 314 – 322, 2012.
- [5] M. Postolski, M. Janaszewski, Y. Kenmochi, and J.-O. Lachaud, “Tangent estimation along 3D digital curves,” in *ICPR 2012*, pp. 2079–2082, IEEE, 2012.
- [6] F. Grélard, F. Baldacci, A. Vialard, and J. Domenger, “Centerlines of tubular volumes based on orthogonal plane estimation,” in *DGCI*, pp. 427–438, 2016.
- [7] M. Couplie, D. Coeurjolly, and R. Zrour, “Discrete bisector function and Euclidean skeleton in 2D and 3D,” *Image and Vision Computing*, vol. 25, pp. 1519–1698, Oct. 2007.
- [8] N. e. a. Cornea, “Computing hierarchical curve-skeletons of 3D objects,” *The Visual Computer*, no. 11, 2005.
- [9] N. D. e. a. Cornea, “Curve-skeleton properties, applications, and algorithms,” *IEEE Trans. VCG*, pp. 530–548, 2007.
- [10] K. Palágyi and A. Kuba, *Directional 3D Thinning Using 8 Subiterations*, pp. 325–336. Berlin, Heidelberg: Springer Berlin Heidelberg, 1999.
- [11] M. S. Hassouna and A. A. Farag, “Variational curve skeletons using gradient vector flow,” *PAMI*, vol. 31, no. 12, pp. 2257–2274, 2009.
- [12] D. Shaked and A. M. Bruckstein, “Pruning medial axes,” *Comput. Vis. Image Underst.*, vol. 69, pp. 156–169, Feb. 1998.
- [13] L. Serino and G. S. d. Baja, “Pruning the 3d curve skeleton,” in *ICPR*, pp. 2269–2274, Aug 2014.
- [14] R. S. Bradley and P. J. Withers, “Post-processing techniques for making reliable measurements from curve-skeletons,” *Computers in Biology and Medicine*, vol. 72, pp. 120 – 131, 2016.
- [15] S. Barbieri, P. Meloni, F. Usai, and R. Scateni, “Skeleton Lab: an Interactive Tool to Create, Edit, and Repair Curve-Skeletons,” in *Smart Tools and Apps in Computer Graphics*, 2015.
- [16] F. Grélard, F. Baldacci, A. Vialard, and J. Lachaud, “Precise cross-section estimation on tubular organs,” in *CAIP*, pp. 277–288, 2015.
- [17] L. Cuel, J.-O. Lachaud, and B. Thibert, “Voronoi-based geometry estimator for 3D digital surfaces,” in *DGCI 2014*, pp. 134–149, 2014.
- [18] “DGtal: Digital geometry tools and algorithms library.” <http://dgtal.org>.